IEEE Access
Multidisciplinary | Rapid Review | Open Access Journal

Received 15 August 2023, accepted 13 September 2023, date of publication 18 September 2023,
date of current version 27 September 2023.

Digital Object Identifier 10.1109/ACCESS.2023.3316508

RESEARCH ARTICLE

A Novel Digital Twin (DT) Model Based on WiFi CSI, Signal Processing and Machine Learning for Patient Respiration Monitoring and Decision-Support

SAGHEER KHAN[1], AAESHA ALZAABI[1], (Member, IEEE), ZAFAR IQBAL[1], THARMALINGAM RATNARAJAH[1], (Senior Member, IEEE), AND TUGHRUL ARSLAN[1,2], (Senior Member, IEEE)

[1]School of Engineering, The University of Edinburgh, EH9 3FF Edinburgh, U.K.
[2]Advanced Care Research Centre (ACRC), The University of Edinburgh, EH16 4UX Edinburgh, U.K.

Corresponding author: Sagheer Khan (s.khan-35@sms.ed.ac.uk)

This work was supported by the Advanced Care Research Centre (ACRC), The University of Edinburgh, Edinburgh, U.K.

ABSTRACT Digital Twin (DT) in Healthcare 4.0 (H4.0) presents a digital model of the patient with all its biological properties and characteristics. One of the application areas is patient respiration monitoring for enhanced patient care and decision support to healthcare professionals. Obtrusive methods of patient monitoring create hindrances in the patient's daily routine. This research presents a novel Respiration DT (ResDT) model based on Wi-Fi Carrier State Information (CSI), improved signal processing, and Machine Learning (ML) algorithms for monitoring and classification (binary and multi-class) of patient respiration. A Wi-Fi sensor ESP32 with Wi-Fi CSI was utilized for the collection of respiration data. This provides an added advantage of unobtrusive monitoring of patient vital signs. The Patient's Breaths Per Minute (BPM) is estimated from raw sensor data through the integration of multiple signal processing methodologies for denoising (smoothing and filtering) and dimensionality reduction (PCA, SVM, EMD, EMD-PCA). Multiple filters and dimensionality reduction methodologies are compared for accurate BPM estimation. The elliptical filter provides a relatively better estimation of the BPM with 87.5% accurate estimation as compared to other bandpass filters such as Butterworth (BF), Chebyshev type 1 Filter (CH1), Chebyshev type 2 Filter (CH2), and wavelet Decomposition (62.5%, 75%, 68.75%, and 75% respectively). Principal Component Analysis (PCA) was performed to provide better dimensionality reduction with 87.5% accurate BPM values compared to EMD, SVD, and EMD-PCA (57%, 44%, and 44% respectively). Additionally, the fine tree algorithm, from the implemented 21 ML supervised classification algorithms with K-fold cross-validation, was observed to be the optimal choice for multi-class and binary-class classification problems in the presented ResDT model with 96.9% and 95.8% accuracy respectively.

INDEX TERMS Digital twin, machine learning (ML), principle component analysis (PCA), respiration rate estimation, signal processing, unobtrusive Wi-Fi sensor.

I. INTRODUCTION

Advancements in technology have drastically transformed our world from time to time. Healthcare has been reshaped into smart and connected healthcare, known as Healthcare 4.0 (H4.0). It is a combination of technologies to create a connection between the digital, physical, and biological spheres. The amalgamation of a variety of technologies, such as Artificial Intelligence (AI) [1], Internet of Things (IoT) [2], [3], Cyber-Physical Systems (CPS) [4], big data [5], [6], etc., are utilized to establish automation and data exchange. Fig. 1. represents the revolution in healthcare. Healthcare 1.0 is at the stage of doctor and patient interactions. The doctor will examine the patient at the clinic and provide

The associate editor coordinating the review of this manuscript and approving it for publication was Ghufran Ahmed.

a diagnosis/medication/care routine based on test results and consultations. Healthcare 2.0 is the implementation of medical devices in monitoring, surgeries, imaging, and life support. Healthcare 3.0 is about utilizing healthcare information technologies to employ computer networks and digitized records to make remote care and telehealth a reality. Creating a gateway between the patient and doctor to replace face-to-face encounters. Being able to do virtual meetings proved to be a major advantage in the recent COVID-19 pandemic. H4.0 is rising in parallel to I4.0 and is proving itself in healthcare to be revolutionary. Healthcare evolved with the use of AI, IoT, CPS, big data, and cloud computing technologies working together [7] to provide a quick and accurate diagnosis of patient big data. Increasing connectivity between the medical equipment and healthcare personnel to enhance patient care, recovery, and experience.

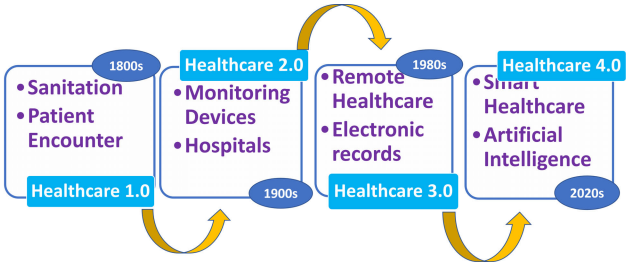

FIGURE 1. Healthcare revolution.

In the last decade, healthcare has kept on improving by providing smart healthcare services. The idea of Digital Twin (DT) has already advanced industries but is going to revolutionize H4.0 [7], [8], [9], [10]. DT allows the formation of a digital representation of the physical system with all its traits. A bi-directional link between the physical system and its digital model [6], [11]. Creating such a link is the task of multiple technologies to work in cooperation with each other. Khan et al. [7] provides a substantial review of such technologies working together for the creation of DT healthcare. The tasks of real-time predictions, comparisons, and simulations of a patient and the environment based on real-time sensor data can become a reality with DT. DT in healthcare can provide early detection of abnormalities, quick and accurate diagnosis, predictive analysis of patient vitals and procedures, the most effective and risk-free surgeries, and improved patient monitoring.

Over the years researchers have worked on implementing DT in healthcare through various methods. H. Laak et al. [12] provided a framework for DT in remote surgeries. To detect abnormalities and diagnosis, an Electrocardiogram (ECG) signal rhythms classifier based on Machine Learning (ML) is implemented [13]. An elaboration of DT in medicine, such as medical CPS, and ML in healthcare is discussed in [14], [15], and [16]. An overview of challenges and technologies in implementing DT in personal healthcare is reviewed in [17] and [18]. Siemens Healthineers optimized Mater Private Hospital (MPH) with the help of DT technology. DT model with AI model was implemented in the radiology department to improve department operations of processing sensor data, patient demands, clinical complexity, and improving infrastructure. Capacity Command Center was designed by GE Healthcare for decision support and simulation capabilities at the John Hopkins Hospital in Baltimore. A DT model of the heart was created by [19]. The human respiratory system was developed by Oklahoma State University's Computational Biofluidics and Biomechanics Laboratory [20], [21], [22]. Most of the healthcare DT models enabled by AI-ML are of humans [23], [24], [25]. According to [26], at this stage, replicating the full functionality of a human is not possible. Thus, the researchers are focusing on utilizing DT on specific aspects of human biology. Fig. 2. represents the multiple application areas of DT in H4.0.

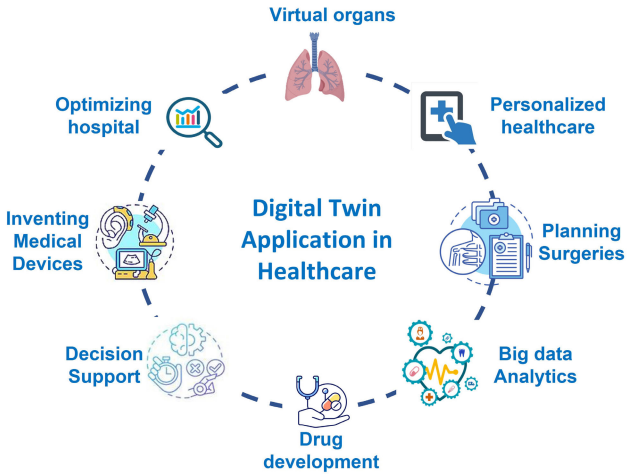

FIGURE 2. DT applications in H4.0.

The paper is distributed in sections for better understanding and improving the layout. Section II provides the motivation and contribution of this research. Section III discusses Wi-Fi sensing and sensing in DT, Section IV is the preliminary discussions on Wi-Fi CSI, PCA, Empirical Mode Decomposition (EMD), and Single Variable Decomposition (SVD), Section V provides an overview of data collection with ESP32 sensor, Section VI is the detailed performance analysis of multiple pre-processing techniques on raw Wi-Fi CSI sensor data in the creation of the ResDT model, Section VII discusses various ML algorithms accuracies for the multiple classification problem, Section VIII discusses the conclusion and future work.

II. PROBLEM STATEMENT AND CONTRIBUTION

A. PROBLEM STATEMENT

Overall, life expectancy has increased, reaching the sixties and beyond. Countries across the world are seeing an increase in their older populations. It is predicted by the World Health Organization (WHO) that by 2030, one out of six people would be 60+ years of age. By 2050, the number of people 60 and older will have doubled [27]. This creates a burden on

the healthcare system and resources [28], [29]. Not only with age, but people of any age can present multiple health conditions with breathing being a crucial indicator of the health condition.

It is elaborated in [30] and [31] that DT in H4.0 has application areas of high-quality economical healthcare, improved patient monitoring, accurate diagnosis and medication, preventing emergencies, and early diagnosis of medical conditions and decision-support. However, it is an open research field with problems of optimal signal processing methodology, how big data analytics can be implemented, which AI and ML algorithms can improve decision-making and predictive analysis, which communication technology is best suited in a specific healthcare scenario, cyber security for sensor and patient data protection, etc. [7].

In [32], around 5% of the population in prosperous countries suffer from the breathing disorder of bradypnea (slow breathing), and nearly 30% of the people in the study, in their 60s, showed symptoms of multiple breathing diseases. In clinical medicine, impedance pneumography, and capnography are two of the conventional methodologies for continuously checking the breathing rate. They are intrusive respiration monitoring methods which may not be considered in the future for elderly care home or hospital environment. Based on the advancements in sensing, signal processing and machine learning, they can be incorporation for enhanced respiration monitoring methodologies.

Unobtrusive sensing methods have a more promising future in healthcare, especially for elderly care. They do not create hindrance in patient daily life as compared to obtrusive methods. Compared to obtrusive data collection, one such solution can be unobtrusive sensor data collection. Liu et al. [24] worked on creating cloud-based DT Healthcare (CloudDTH) for real-time monitoring of the patient. The data acquired through the ECG sensors are sent to the CloudDTH platform through the ECG device (Huake HKW-10). The authors presented a contact based DT model for data collection. Jagade et al. [33] worked on monitoring human respiration rate through Infrared Thermography (IRT) but that requires clear LOS between the infrared camera and the patient. Chu et al. [34] monitored the respiration rate of the human through low-powered piezo-resistive sensors attached to the human body. The sensors are combined with Bluetooth units to observe respiration rate from a distance but the sensors can create hindrance in daily routines. Ryser et al. [35] utilized a single chest-worn accelerometer to estimate the respiration rate. Respiration and abdominal bands are attached on the around the chest. Even with unobtrusive sensing methods, there is the limitation of clear LOS, privacy concerns, or the need of putting on special equipment by the patient.

In the above-mentioned literature along with the work presented in [36], [37], and [38], they have the limitation of obtrusive sensing, the need for clear LOS, and restricts the patient's movements. Hence, unobtrusive sensor data collected with Wi-Fi CSI can provide a better solution for unobtrusive monitoring of the patient/elderly vital signs without the need for clear LOS, no privacy violation, or the need for special arrangements. Wi-Fi CSI has the advantage of monitoring the patient's physical, physiological, and biological features without the technology creating obstruction in the daily routine.

B. CONTRIBUTION

Following are the novel points of this research toward implementing DT technology in healthcare for monitoring the Breaths Per Minute (BPM) of a patient with respiration problems through unobtrusive Wi-Fi sensing with integration of signal processing methodologies and ML algorithm.

1) We propose a novel DT model (ResDT) based on Wi-Fi CSI for patient respiration rate. ESP32 sensor with Wi-Fi CSI allows for an unobtrusive method of respiration data collection for the DT model.
2) Our study is the investigation of signal processing techniques performance analysis comparison on complex noisy ESP32 sensor data in the proposed ResDT model. This will help select the optimal methodology for estimating accurate BPM from raw sensor data. Various techniques comparison comprise; multiple Infinite Impulse Response (IIR) bandpass filters (0.15Hz to 0.6Hz) and wavelet decomposition performance comparison for denoising the respiration sensor data; multiple dimensionality reduction methodologies comparison on complex Wi-Fi CSI respiration datasets in the estimation of the patient's BPM.
3) In our research, 21 ML-based supervised learning classification algorithm accuracies, along with K-fold cross-validation, are assessed for the various classification problem of abnormal and normal respiration rates in the proposed ResDT model. This will help in implementing decision-support or classification between binary and multi-class problems in proposed ResDT model.

C. PROPOSED ResDT MODEL

Fig. 3 represents the proposed Respiration DT (ResDT) model. ESP32 Wi-Fi sensor with CSI characteristics collects patient respiration data unobtrusively. The raw data is not ready to analyzed for the estimation of the patient's BPM. It is subjected to multiple denoising methodologies of smoothing, bandpass filters, and PCA to acquire the patient BPM from raw sensor data. Feature data is extracted, enabling the testing of ML algorithms and neural networks for binary and multi-class classification in the proposed ResDT model.

III. SENSING

A. Wi-Fi SENSING

The recent COVID-19 pandemic has shown how conventional methodologies fail in providing healthcare in such harsh conditions [39], [40]. Not only that, with the increasing number of elderly patients, it is important to look for new innovative noninvasive techniques to overcome these

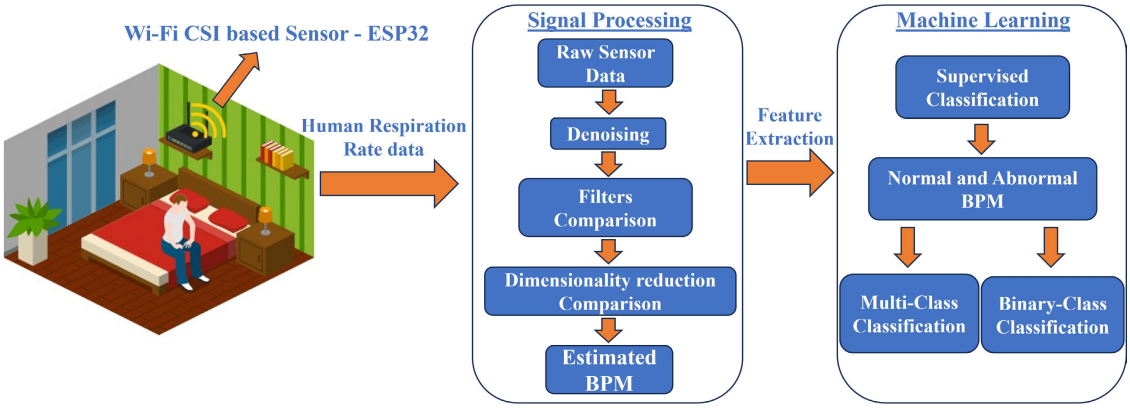

FIGURE 3. ResDT: proposed respiration DT model with ESP32 sensor.

challenges. Researchers can make use of cameras indoors to capture images of respiration signals [41]. The major drawback of this camera-based respiration monitoring is that the images require a clear line of sight and sufficient illumination [42], [43]. An additional drawback is that the cameras are a privacy concern. Under the threat of cybercrimes, it is difficult to have a promising solution for indoor sensing [44]. Wearable devices can be utilized as a solution for unobtrusive sensing [45]. Even though wearable devices have a broad range of applications, they need exclusive gear to be worn for extended periods and are only appropriate for extended periods of monitoring an immobile patient [46]. A smartphone can be a solution to acquire data from the subject's body but it needs to be carried all the time [47], [48]. Another solution can be the environmentally installed sensors but they require a heavy installment setup [49], [50].

A real-time economical unobtrusive respiratory monitoring method is essential. Wi-Fi sensing can be utilized to sense the vital signs of a patient from a distance [51], [52]. But recent studies have shown that Wi-Fi signals tend to get disturbed by the movement of residents and other movements in a zone [53]. For that, in Wi-Fi sensing data, Channel State Information (CSI) [54] applies to a range of applications such as sedentary behavior analysis [55], gesture recognition [56], vital sign detection [57], human detection [58], occupancy detection [59], crowd counting [60], and human activity recognition [61], etc. Compared to contact-based sensing methods, Wi-Fi signals have multiple excellent attributes and advantages over wearable devices.

1) Only information about the human vital signs, position, etc. can be obtained from the wireless signals. Wi-Fi signal protects the user's privacy as it cannot acquire details about appearance, clothes, etc.
2) Wireless-based sensing technology does not require specific gears to be worn by the user. It still achieves accurate sensing and is very appropriate for long-term implementation.
3) Wireless signals are propagated in a zone and do not depend upon LOS. Diffraction and reflection of wireless signals can still deliver valuable sensor data even if there is an obstruction in the middle of the device and the user.
4) The wireless signal transmission and reception do not depend on the light, making it possible to work around the clock.

B. SENSING IN DT

Wi-Fi sensing is not only important for the unobtrusive respiration monitoring of a patient but also crucial in the creation of DT models. The DT's popularity increased with the availability of economical and miniature-size sensors that can provide all kinds of patient vital information. These models are data-driven and can only represent the theoretical behavior of a system if the actual state in the physical world is unknown. The choice of the sensor itself is critical as it impacts the functionality and accuracy of the DT model. Khan et al. [44] discussed the importance of the sensor's position in data collection for the creation of DT models. If the sensor utilized provides inaccurate measurements of the patient's respiration rate, the DT model will not replicate the respiration behavior in real-time. This will lead to inaccurate recommendations with the DT utilized in research or clinical trials.

In the context of DT technology in healthcare, unobtrusive sensing through Wi-Fi CSI has a vital role in building an accurate DT model that reflects the current state of the patient. The benefits of data sensing in DT include predictive analysis, equipment maintenance, optimizing healthcare, accurate real-time monitoring, and improved decision-making. Unobtrusive Wi-Fi sensing with outstanding characteristics gives it a broad range of potential applications in DT and the possibility to be the cornerstone of the following generation of sensing technology.

IV. PRELIMINARIES

A. CHANNEL STATE INFORMATION (CSI)

Numerous wireless network standards e.g., LTE, Wi-Fi, and WiMAX embrace Orthogonal Frequency-Division Multiplexing (OFDM) for communication [62]. OFDM is the

suitable choice for achieving high data rates and frequency-selective channels. The total spectrum is split into narrowband orthogonal subcarriers in OFDM. The channel fading caused by large delay spreads is lessened by the utilization of Inverse Fast Fourier Transform (IFFT) for data transmission on the subcarriers. The complexity of the Fast Fourier Transform (FFT) at the receiver can be reduced by the utilization of cyclic redundancy. Channel properties of the communication link between the transmitter and receiver are represented by the CSI. It can be freely acquired from the signals of COTS Wi-Fi devices equipped with a Network Interference Card (NIC). The CSI signals are the superpositions of the signals from different propagation paths. The outcome of analyzing the CSI is that the information of the surrounding, encoded in the Wi-Fi signals, can be acquired. The CSI has been measured at different subcarrier frequencies due to the OFDM. Multiple antennas are authorized to communicate through multiple data streams in a Multiple-Input Multiple-Output (MIMO) system. The propagation of a Wi-Fi signal can be affected by the micro-movement of the subject. The kind of micro-movement under observation in this research is respiration. This can thus be detected by CSI. Bao et al. [63] provide a discussion on the phase and amplitude changes toward detection of such micro respiration movements. Mathematically, the signal at the receiver can be stated as a function of the transmitted signal [64].

$$y_i = H_i x_i + n_i \tag{1}$$

The transmitted signal is represented by $x_i = R^{(N_T)}$ and the received signal is represented by $y_i = R^{(N_R)}$. The subcarrier index is represented by i whereas, n_i is the noise vector. N_T represents the number of the transmitter antenna. N_R are the number of receiver antenna. $H_i \in \mathbb{C}^{(N_R x N_T)}$ represents the complex CSI matrix.

$$H_i^{mn} = \begin{bmatrix} H_i^{11} & H_i^{12} & \dots & H_i^{1N_T} \\ H_i^{21} & H_i^{22} & \dots & H_i^{2N_T} \\ \dots & \dots & \dots & \dots \\ H_i^{N_R1} & H_i^{N_R2} & \dots & H_i^{N_RN_T} \end{bmatrix} \tag{2}$$

For the communication link, between the $n-th$ transmitter antenna and $m-th$ receiver antenna, H_i^{mn} is the channel frequency response.

$$H_i^{mn} = |H_i^{mn}| + \exp(j\angle H_i^{mn}) \tag{3}$$

$\angle H_i^{mn}$ and $|H_i^{mn}|$ correspond to the phase and amplitude response.

B. PRINCIPAL COMPONENT ANALYSIS (PCA)

The complexity of high-dimensional sensor data is simplified while preserving trends and patterns by using PCA. PCA retains information as much as possible from the original signal while deriving the data signal into a fewer number of decorrelated linear combinations. The general idea of PCA is to find the Principal Components (PC) of the data signals that are orthogonal to each other [65]. PCA can be utilized in multiple applications e.g., data compression, noise reduction, biological signal processing [66], and image and pattern recognition [67], [68], [69]. Some of the PCA advantages are:

1) Lower memory requirements.
2) Orthogonality decreases the absence of repetition in the data by utilizing orthogonal components [70], [71].
3) Noise reduction as the maximum variation basis is considered. In the background, the small variation is automatically removed [70].
4) Reducing complexity as data is grouped by the PCA [70], [71].
5) PCA does not require complex computations.

However, in the PCA, until the training data provides specific information, the simplest invariance could not be captured [72]. Also, it is difficult to compute the covariance matrix accurately in PCA [70]. Khanh et al. [73] utilized Ultra-Wide Band (UWB) impulse radar to sense the vital signals of the heart rate of the patient. The data is subjected to PCA for reducing data complexity and acquiring the projection on the primary PC. Such a projection facilitates substantially enhancing the Signal-to-Noise (SNR) in comparison to other techniques of complex signal decomposition and Direct Fast Fourier Transform (DFFT). PhotoPlethysmoGraphy (PPG) signals can be utilized to obtain cardiorespiratory signals i.e., respiration rate and heart rate which will lessen the number of sensors placed on the patient's body for data collection [74]. The authors proposed Ensemble Empirical Mode Decomposition with Principal Component Analysis (EEMD-PCA) for estimating heart rate and respiration rate concurrently from the PPG datasets of MIMIC (Physionet ATM data bank) and Capnobase database with the short length of 30 seconds. The proposed algorithm provided better results compared to existing methods of Correntropy Spectral Density (CSD) [75], Power Spectral Density (PSD) [75], Smart Fusion [76], and Empirical Mode Decomposition (EMD) [77]. Another example of recent work of respiration rate estimation based on Wi-Fi frame capture [78]. The authors worked on Beamforming Feedback Matrices (BFMs) contained in the capture frames. BFM is a rotated matrix of CSI. PCA was utilized to separate the data from the chest movements of the subjects in the BFMs. The resulting data were subjected to Discrete Fourier Transform (DFT) to estimate respiration rates in the frequency domain. It is stated by the authors that the frame-capture-based respiration estimation has a lower estimation error than 3.5 breaths/minute.

1) MATHEMATICAL MODEL

Details of mathematical model of PCA is discussed in [79] and [80] but the following mathematical model provides a generic overview of how PCA works in our dataset. The input matrix X of time series respiration sensor data is represented

in Equation 4:

$$X_(t) = [x_1(t) + x_2(t) + x_3(t) \ldots .. + x_n(t)] \quad (4)$$

The respiration signals are obtained from raw sensor data by using the PCA through the covariance matrix. The covariance matrix is defined as Equation 5 or Equation 6:

$$C = conv(X) \quad (5)$$

Or,

$$C = \frac{1}{n} \sum_{j=1}^{n} X_j X_j^T \quad (6)$$

This provides an $m * m$ matrix. The answer to Equation 7 provides the eigenvector α_j and eigenvalues λ_j.

$$C_j \, \alpha_j = \lambda_j \, \alpha_j \qquad j = 1, 2, 3, 4, \ldots .n \quad (7)$$

The PCA acquired are using Equation 8:

$$z_j = \alpha_j \, X \quad (8)$$

They are assembled in order of magnitude of eigenvalues. The eigenvalues correspond to the fraction of the total variance. So, the PC with the most variance is considered the signal with the most data.

C. EMPIRICAL MODE DECOMPOSITION (EMD)

EMD is a data-driven signal processing technique that obtains the oscillatory tones embedded in a signal. No prior knowledge of the data is necessary, thus making it fully data-driven. EMD or Hilbert-Huang Transform decomposes multi-component, nonlinear signals into oscillatory modes of the signal called Intrinsic Mode Functions (IMFs) and a monotonic function known as residue [81], [82]. The shifting process, an iterative process, is utilized to estimate the IMFs [83].

$$X(t) = \sum_{i=1}^{M} C_i(t) + r_M(t) \quad (9)$$

$X(t)$ represents the discrete-time samples. Where in $C_i(t)_{i=1}^{M}$, M is the number of obtained IMFs with the same length as $X(t)$. Residue function is presented by $r_M(t)$.

EMD has been used for some time in multiple engineering areas, including denoising ECG signals, classification of EEG, and various biomedical engineering fields. The output of the EMD is the variable quantity of components that have the same length as that of the original signal. Researchers have been using EMD for the estimation of patient vital signs. Pinheiro et al. [84] utilized EMD and PCA to acquire patient's cardiovascular vitals from raw data of a chair-based system. The performance of EMD for respiration vitals estimation in [85] and [86].

In our research, we aim to utilize EMD as a dimensionality technique methodology with IMFs being utilized to estimate the patient's BPM for the creation of a respiration DT model.

D. SINGLE VARIABLE DECOMPOSITION (SVD)

SVD is a characteristic decomposition and massive data compression technique utilized in the fields of data analysis, ML, and signal processing. SVD disassembles the sensor data matrix into three components: U (left singular vector), Σ, and V (right singular vector). The U and V are the orthogonal matrices, whereas, Σ is the singular values of the original matrix represented in a diagonal matrix. Liu et al. [87] provided a detailed mathematical model of SVD for signal processing. According to [88], a simpler version can be represented in equation 10:

$$A = U * \Sigma * V^T \quad (10)$$

where A is an MxN matrix, U is an MxM, Σ is an MxN matrix, and V^T is an NxN matrix.

In our research, the purpose of the SVD method is to achieve denoising, dimensionality reduction, and characteristic decomposition to estimate the patient's BPM for the creation of a respiration DT model.

V. RESPIRATION DATA COLLECTION WITH ESP32

ESP32 Microcontroller units containing Wi-Fi modules using the esp32-CSI tool have been utilized to collect datasets i.e., Wi-Fi sending data using CSI for respiration rate measurements, in a standard 3m x 3m room [89]. With respect of Fig. 3, this is the initial stage where patient respiration data collection is performed with ESP32 sensor. The patient chest expansion and contraction during the breathing process perturbs the Wi-Fi's propagation environment. The chest small perturbations are detected as small changes in the Wi-Fi CSI data [90]. The Wi-Fi CSI-based non-invasive sensor datasets are collected from the experiments to be utilized for creating a patient DT model. The experiment was performed with the Wi-Fi transmitter and receiver in a 3m x 3m room. The subject is seated around 0.9m perpendicularly from the midpoint of the transmitter-to-receiver direct line-of-sight distance away from the Wi-Fi transmitter and receiver, which were installed at a height of 0.85m from the floor level. The subject's age is 26; 1.56m tall and weighs 47kg. Sensor data is collected over 2 minutes with 120 packets per second sampling rate of the transmitter. The sensor data is expected to be 14400 packets according to the sampling rate, but it is expected in the experimental setup to have losses. The sensor data has 52 subcarriers as the sensor with Wi-Fi CSI characteristics utilizes the concept of OFDM. The beats are set to a range of 12BPM to 28BPM to depict the respiration rate of older adults. The range of normal BPM for older adults is 12 to 16 and beyond which is an indication of health problems. MATLAB has been used to acquire Wi-Fi CSI signal from the .csv file, signal processing, and utilizing ML algorithms for BPM rate calculation, classification of normal and abnormal BPM, and predicting BPM values. Fig. 4 represents the Wi-Fi CSI respiration rate data collection of a patient with an ESP32 sensor.

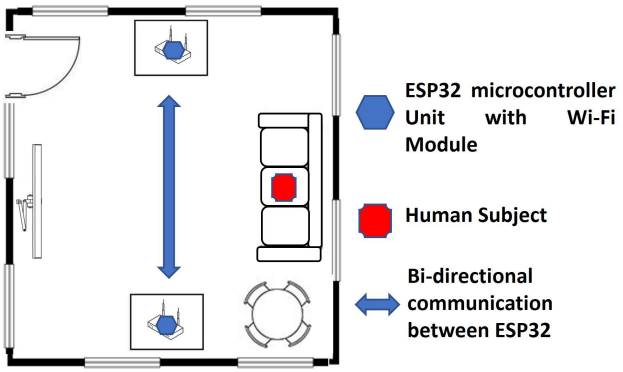

FIGURE 4. Wi-Fi CSI respiration rate data collection in a room.

VI. RESPIRATION DT MODEL PRE-PROCESSING

A. METHODOLOGY AND FILTERS COMPARISON

Filtering is the central part of extracting the respiration signal from a strong noisy signal. It is attained by utilizing capable bandpass digital IIR filters. In [33] and [91], the authors provided a comparison of IIR and FIR filters for baseline noise removal in the ECG signals. Due to the computational complexity of FIR, higher memory requirements, and phase delay due to higher-order FIR, IIR is considered a better option. Fig. 5. provides an overview of the methodology adopted for pre-processing raw Wi-Fi CSI data for estimating patient BPM.

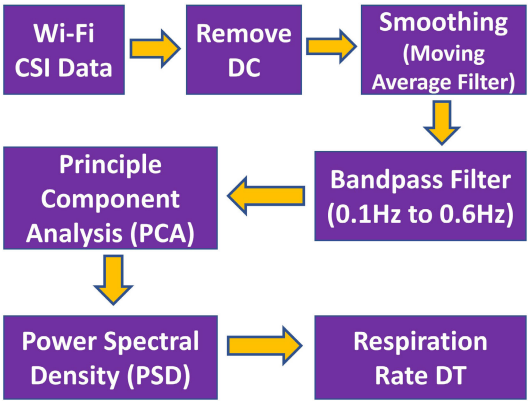

FIGURE 5. Block diagram of pre-processing raw respiration Wi-Fi CSI data.

In this research, we aim to utilize bandpass digital IIR filters for acquiring the appropriate frequency range (0.1Hz to 0.6Hz) for respiration rate from the noisy Wi-Fi CSI sensor data. A comparison of multiple IIR filters and wavelet decomposition method is additionally carried out. The following are compared in terms of acquiring accurate BPM from raw sensor data:

1) Butterworth Filter (BF)
2) Chebyshev type 1 Filter (CT1F)
3) Chebyshev type 2 Filter (CT2F)
4) Elliptic Filter (EF)
5) Wavelet Decomposition

TABLE 1. Respiration rate of multiple IIR filters.

CSI Data	Butterworth	Elliptic	Chebyshev1	Chebyshev2	Wavelet
12BPM	12	12	13	12	12
13BPM	15	15	15	15	13
14BPM	7	15	18	18	14
15BPM	9	14	15	9	13
16BPM	18	14	21	21	20
17BPM	22	22	22	22	11
18BPM	21	16	21	21	18
19BPM	22	21	22	22	19
20BPM	24	24	24	24	19
21BPM	10	25	10	10	21
22BPM	24	24	24	24	12
23BPM	27	21	27	27	20
24BPM	29	10	29	29	12
25BPM	8	23	21	29	18
26BPM	12	30	34	10	26
27BPM	7	10	19	9	29
28BPM	33	30	10	33	28

Table. 1 provides a comparison of multiple IIR filters and wavelet decomposition for the calculated BPM after pre-processing. The resulting data from each of the methodology is passed through the PCA for respiration rate estimation. The elliptic filter provides the least number of errors in calculating the BPM concerning the inter-observer variability threshold of $+-5$ BPM [92], [93], [94]. The elliptical filter provides a relatively better estimation of the BPM with 87.5% accurate estimation as compared to other bandpass filters such as Butterworth (BF), Chebyshev type 1 Filter (CH1), Chebyshev type 2 Filter (CH2), and wavelet Decomposition (62.5%, 75%, 68.75%, and 75% respectively). Additionally, for normal BPM (12 to 16), elliptical filter presents no inaccurate calculation of the BPM based on the inter-observer variability threshold.

B. ELLIPTIC FILTER PARAMETRIC ANALYSIS

Table. 2 represents the values of metrics such as SNR, Peak Signal-to-Noise Ratio (PSNR), and Shannon entropy for all the experimental and pre-processed BPM signals. This provides a performance overview of the pre-processing methodology implemented to acquire the subject respiration information from raw sensor data. The SNR values are shown for both the raw and the pre-processed signal. It indicates an increase in signal strength with the pre-processing methodology implemented. PSNR is the ratio of the maximum possible value of a signal and the noise level. PSNR is interpreted as the higher the value, the better the quality of the signal. According to Table. 2, the PSNR provides positive values for all the BPM showing a positive signal strength over the noise. The Shannon entropy is considered a natural choice for quantifying the complexity of a signal. Higher entropy represents higher uncertainty and a more unpredictable signal. Shannon entropy is considered for the raw and pre-processed signal. According to Table 2, for the majority of the signals, there is an increase in entropy value after pre-processing is applied to the raw signal. A higher

TABLE 2. Signal parametric analysis before and after pre-processing with elliptic filter.

BPM	SNR-Raw	SNR-Processed	Entropy-Raw	Entropy-Processed	PSNR
12	0.16	4.51	4.57	12	5.01
13	0.67	3.56	3.52	15	6.04
14	2.10	8.57	3.90	18	8.40
15	0.84	5.20	4.5	9	3.58
16	0.51	9.96	3.93	21	4.48
17	1.03	15.72	3.96	22	7.39
18	0.18	6.43	4.21	21	2.93
19	0.66	3.88	4.44	22	2.54
20	0.07	8.29	4.53	24	2.67
21	0.57	2.58	4.33	10	1.80
22	0.84	8.30	3.34	24	4.08
23	1.17	7.99	3.38	27	7.47
24	0.37	3.61	3.32	29	5.42
25	0.09	11.31	3.47	29	4.04
26	0.75	8.62	4.84	10	0.61
27	1.59	10.42	4.28	9	4.3
28	0.45	10.95	4.28	33	4.30

entropy can be an indication of pre-processing adding noise or complexity to raw sensor data. However, the BPM values acquired for the majority of the sensor data are within the inter-observer variability threshold of $+-5$.

C. STEP-BY-STEP PERFORMANCE ANALYSIS

Fig. 6 provides the results throughout the multiple stages of pre-processing presented in Fig. 5. Following is the step-by-step detail elaboration of the pre-processing output:

1) Fig. 6(a) is the raw 12 BPM Wi-Fi CSI sensor data considered as an example of pre-processing techniques. The DC offset is removed from the sensor data set by subtracting the mean from it, Fig. 6(b).
2) The sensor data is then subjected to a smoothing process i.e., the moving average [32] in Fig. 6(c). Smoothing is implemented to discover important patterns in data while removing the unnecessary information (i.e., noise).
3) The smoothed data is passed through the bandpass filter (frequency range 0.1Hz to 0.6Hz [73], [76], [77]) shown in Fig. 6(d). A bandpass filter allows the signal in a specific band of frequencies, called a passband but blocks the components with frequencies above and below the band. This is a contrast to the high pass filter and low pass filter, which allows the components above and below the specific frequencies, respectively. An ideal bandpass filter will have a completely flat passband with all the frequencies passing to the output without attenuation or amplification and complete attenuation for frequencies outside the passband. But achieving an ideal bandpass filter is not possible in the real world.
4) As for dimensionality reduction, by using PCA, the processed data is projected in the form of principal components. The total number of principal components is 52 presented in Fig. 6(e).
5) A scree plot has been used to visualize all the principal components of the filtered CSI signal. This will help in deciding which PC to retain and which to let go of. The PCs of the data signal will have variable variance. PC1 will have the highest variance, PC2 with the second highest variance, and so on. No definite rule is present for deciding when to stop including the variables but in [95], two recommendations are provided. The first recommendation is to select stop selecting the variables when an elbow in the scree plot appears - the plot begins to flatten out. The second recommendation is to stop selecting the variables when the variable falls below 1. Yu et al. [96] provided a discussion in terms of the bandpass filter and PCA. With the bandpass filter removing the noise, this allows the PCA to maximize the amplitude of the signal rather than the noise. The authors calculated the scree plot and selected the first PC component since it has the highest variance. Based on the discussion of [95] and [96] and according to the scree plot of Fig. 6(f)., the first PC will be selected to calculate the BPM of the patient.
6) The first PC is represented in Fig. 6(g). The final stage is to implement the Power Spectral Density (PSD). It is the method of characterizing the distribution of the signal frequency components in an easier visual interpretation than a complex Discrete Fourier Transform (DFT) [95].
7) Fig. 6(h) represents the PSD graph has a frequency, with the maximum power, 0.205 is multiplied by 60 to acquire 12.3 BPM. According to [92], [93], and [94], the clinical limits can be defined as $+/-$ 5 BPM, or the inter-observer variability in the clinical setting can result in a BPM difference between 2 to 5 BPM.

D. COMPARISON OF MULTIPLE TECHNIQUES AND ResDT MODEL

In our research, we aim to perform a comparison to analyze the suitability of multiple techniques such as EMD, PCA, EMD-PCA, and SVD in the development of the ResDT model. The elliptic filter will be used as a bandpass filter in comparison to EMD, PCA, EMD-PCA, and SVD. EMD-PCA is a modification to the initial EMD method. This offers a harmonious approach toward denoising and finding out prominent features in raw sensor data. EMD applied as a pre-processing step, generates IMFs. These IMFs are further analyzed by PCA to identify the most relevant IMFs and extract their corresponding features. The combination of these techniques allows for extracting salient features, a robust framework for denoising, and a compact and meaningful representation of data.

Table 3 provides a comparison between EMD, PCA, EMD-PCA, and SVD in terms of estimation of the patient BPM. According to the interobserver variability of $+-5$BPM, PCA provides the least errors in BPM estimation as compared to other methodologies. Incorrect BPM estimations are presented as bold in Table 3. PCA is the suitable option

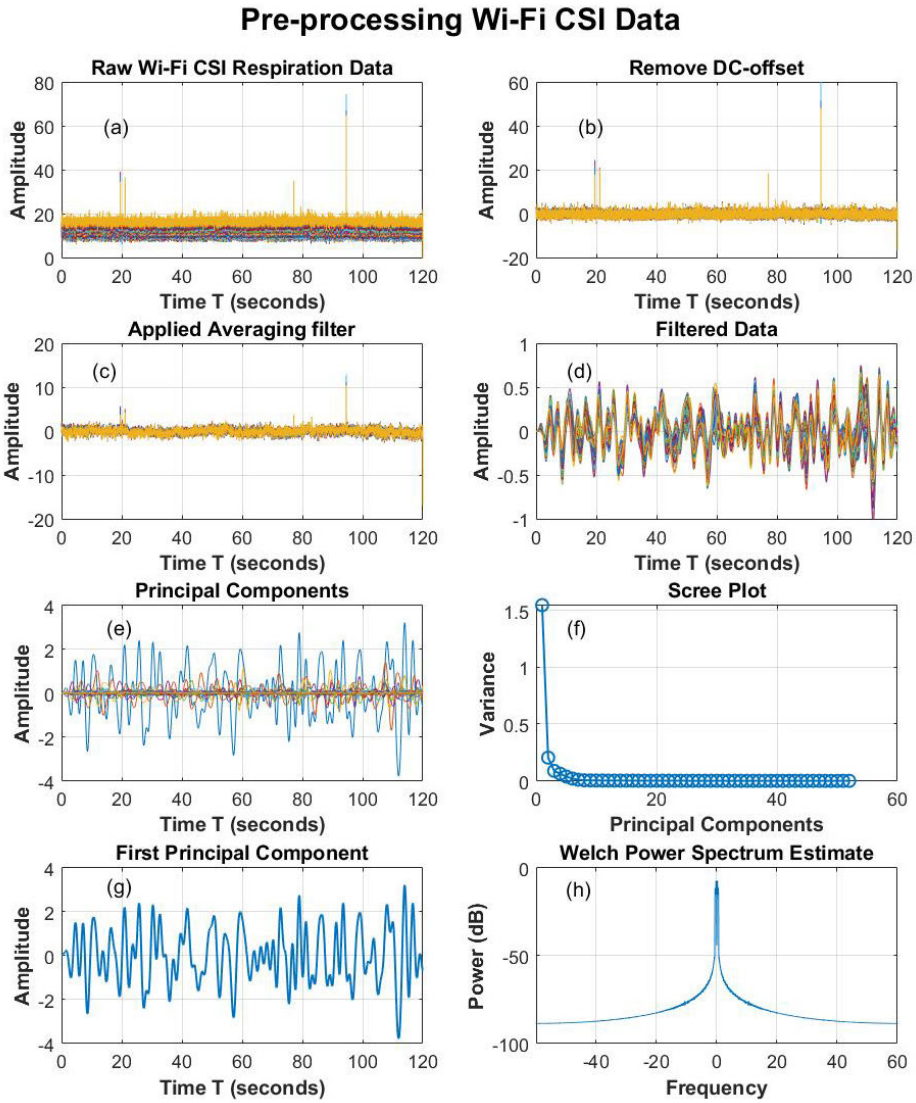

FIGURE 6. Pre-processing of raw respiration Wi-Fi CSI data (a) Raw respiration Wi-Fi CSI data (b) DC-off set removed from respiration Wi-Fi CSI data (c) respiration Wi-Fi CSI data after moving average filter (d) Respiration Wi-Fi CSI data after Elliptical bandpass filter (e) All principal components after PCA (f) Scree plot (g) First Principal Component (PC1) (h) PSD of First Principal Component.

to be utilized as a pre-processing methodology for the respiration data acquired through ESP32 unobtrusive sensor. The resulting BPM through the PCA is presented in Fig. 7 as a respiration DT model, ResDT.

Similar to [24], the ResDT model will be presented in the form of a estimated BPM graph. The BPMs are recorded by the subject in a linear format starting from 12BPM to 28BPM. The respiration data is currently from a single subject to create the ResDT model. It is performed on purpose to know that the data collected can be labeled a certain BPM for the implementation of supervised ML. The ResDT model is represented in Fig. 7. According to the interobserver variability of $+-5$BPM, the least number of experimental BPM (15, 21, 27) is incorrectly estimated after applying the pre-processing methodologies.

VII. MULTI-CLASS AND BINARY-CLASS SUPERVISED CLASSIFICATION FOR ResDT MODEL

Various combinations of generic data processing techniques precede ML classification and regression processes before the respiration rate DT. Pre-processing is the first stage before any ML implementation in terms of learning and understanding depending on the features [97]. Some of the recent research work involves the utilization of ML algorithms for the accurate prediction of numerous medical methodologies with real-time data and processing capability [98]. Lee et al. [15] elaborated on a context-aware healthcare system using the DT framework. ECG-based rhythms classifier model is created with ML to detect cardiac problems and diseases. In [99], authors utilized ML algorithms to accurately measure the bio-signals.

TABLE 3. Comparison based on BPM estimation.

CSI DATA	EMD	PCA	SVD	EMD-PCA
12 BPM	12	12	12	12
13 BPM	14	15	18	14
14 BPM	17	15	**10**	18
15 BPM	**9**	14	**10**	**10**
16 BPM	21	14	**8**	**8**
17 BPM	17	22	17	18
18 BPM	21	16	21	21
19 BPM	22	21	22	22
20 BPM	21	24	21	**30**
21 BPM	**33**	25	**33**	**30**
22 BPM	**10**	24	**14**	**14**
23 BPM	19	21	19	19
24 BPM	**10**	**10**	**10**	**10**
25 BPM	21	23	21	21
26 BPM	**12**	30	**12**	**12**
27 BPM	**19**	**10**	**10**	**19**
28 BPM	**12**	30	**22**	**22**

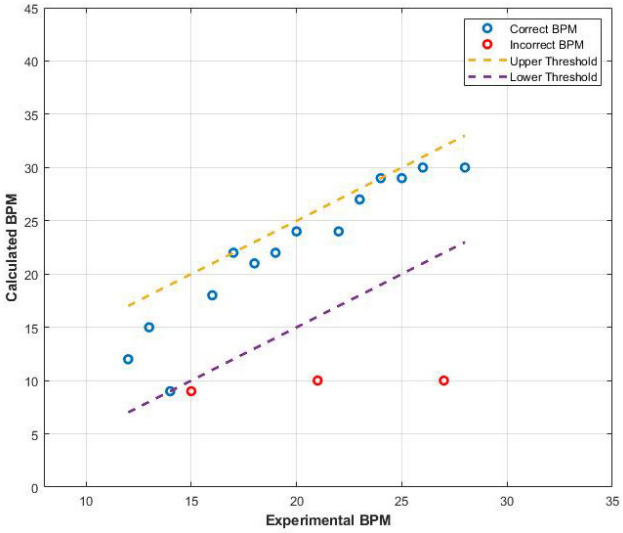

FIGURE 7. ResDT of the patient's BPM.

In our research, the focus is to utilize numerous ML based algorithms for supervised classification in the ResDT model. This will help analyze the suitability of of algorithms, classification problems, and understanding toward a multi-patient hospital DT model.

A thriving DT healthcare model depends on effective and precise ML algorithms to accurately perform multiple processes. Pre-processing has its importance. The signal-to-noise ratio is improved by pre-processing, which directly impacts the decision-making ability of the ML model for classification and regression. Data heterogeneity, data redundancy, and noisy data are some of the problems with ML implemented directly on raw datasets [100]. Experimental data is of a single subject over 2 minutes for every BPM. However, to increase the size of the data, the data is split into 30 secs. The features selected are of, according to Fig. 6(h), frequency and power value. The frequency value selected will correspond to the highest power value in that PSD for those specific 30-sec data selected. The total data size for ML

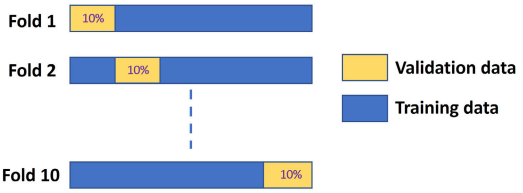

FIGURE 8. 10-fold cross-validation in ResDT model.

is 408 BPM values. This will help analyze the ML algorithm's accuracy in the ResDT model in terms of how successful they are in the classification of a certain BPM value (abnormal or normal) if continuous 30 secs pre-processed data is provided as input. The data is shuffled, and the total data set is kept at 80% training and 20% test datasets respectively. The training dataset is split into training and validation data sets. For validation, the k-fold cross-validation method is utilized [33]. The purpose of the validation data set is to provide an estimate of the model skill. The capability of the ML model on an unseen data sample is estimated by utilizing the statistical method of cross-validation. Cross-validation 10-fold is used in our ML ResDT model. Fig. 8 provides a representation of the 10-fold cross-validation for ML algorithms in the ResDT model.The validation set will be considered as the first fold, and the remaining n-1 folds (n=10 here) will be utilized for fitting the model and then the second fold and so on.

A. CLASSIFICATION ANALYSIS

Table 4 provides the accuracies of multiple classification algorithms on the calculated BPM, pre-processed raw Wi-Fi CSI data, of the ResDT model. These 21 algorithms are utilized for supervised learning classification problems. MATLAB classification learner app allows for built-in classifiers. Overall, these algorithms are a strong starting point for many supervised learning problems with a range of techniques that can be adapted for many different types of applications and data. Table 4 provides the binary-class and multi-class classification accuracies of the 21 supervised classification algorithms. The ML algorithms have to classify the abnormal BPM(17BPM to 28BPM) and normal BPM(12BPM to 16BPM). In multi-class classification, the ML algorithms have to classify between 13 different BPM ranging from 12BPM to 28BPM. Free Tree algorithm has the best accuracies of 96.9% and 95.8% for multi-class and binary-class classification respectively in the proposed ResDT model. A comparison in terms of classification can be carried with [64]. Hu et al. utilized the Convolutional Neural Network (CNN) on respiration Wi-Fi CSI sensor data for classification problems to show the potential of learning-based algorithms in unobtrusive vital sign detection. Our proposed ResDT has multi-class and binary-class classification accuracies of with 96.9% and 95.8% respectively compared to [64] 96.05%. Additionally, the classification is performed on 16 different classes as compared to [64] 6 classes.

TABLE 4. ML and DL algorithms accuracies for DT model.

Algorithm	Multi-Class Accuracy%	Binary Class Accuracy%
Fine tree	96.9	95.8
Medium tree	95.9	92.8
Coarse tree	70.2	93.8
Linear SVM	93.9	84.4
Quadratic SVM	90.2	84.4
Cubic SVM	90.5	77.9
Fine Gaussian SVM	82.2	89.8
Medium Gaussian SVM	93.6	90.8
Coarse Gaussian SVM	89.9	84.4
Fine KNN	89.6	91.8
Medium KNN	80.4	92.8
Cosine KNN	58.6	90.8
Cubic KNN	78.2	92.8
Weighted KNN	88.3	93.8
Bagged trees–Ensemble	96.1	94.8
Subspace discriminant–Ensemble	80.6	84.4
Subspace KNN–Ensemble	68.1	93.8
Narrow NN	92.3	91.8
Medium NN	93.6	94.8
Wide NN	94.2	93.8
Bilayered NN	92.6	94.2

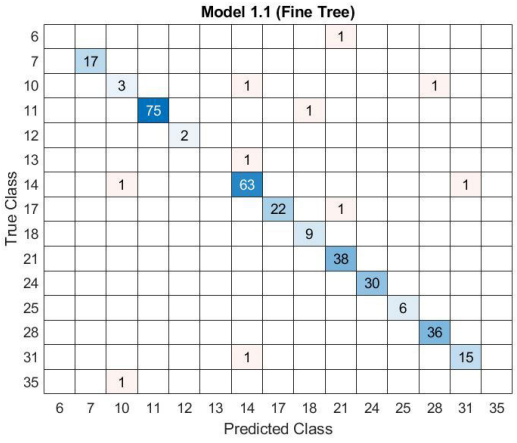

FIGURE 9. Confusion matrix of fine tree algorithm for multi-class classification.

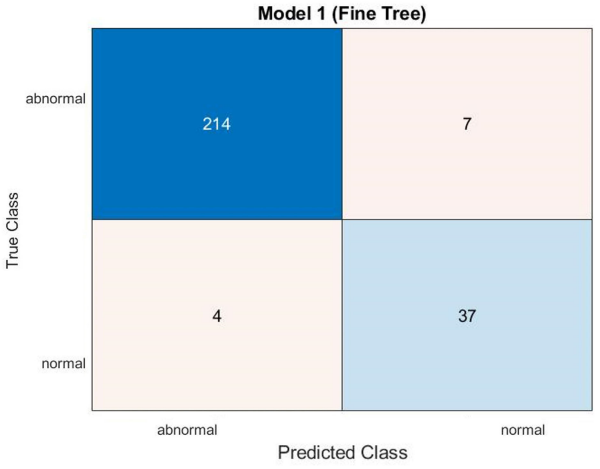

FIGURE 10. Confusion matrix of fine tree algorithm for binary-class classification.

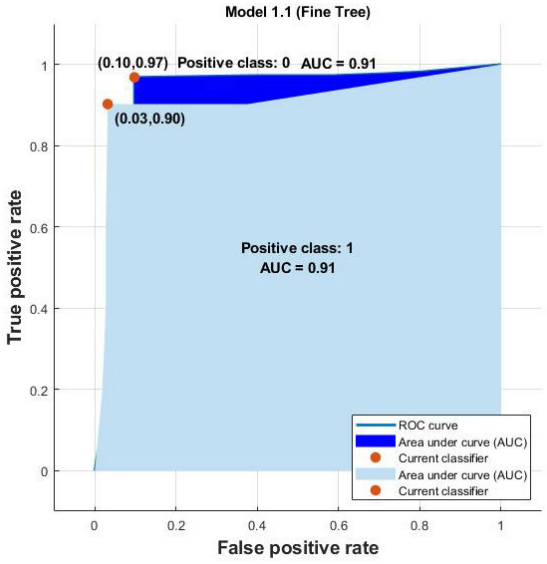

FIGURE 11. ROC and AUC curve for binary classification problem of normal and abnormal BPM for Fine Tree algorithm.

The confusion matrix of the fine tree algorithm for multi-class and binary-class classification is Fig. 9 and Fig. 10. According to [101], The k-fold cross-validation method is considered to have the strongest bias performance estimates with a small data set. The authors performed a comparison with multiple validation methods in terms of bias ML performance estimation.

For binary classification, a metric of performance analysis is the Receiver Operating Characteristic (ROC). The ROC is the relationship between the True Positive Rate (TPR) and the False Positive Rate (FPR) for the different threshold values applied to classify the data. Whereas the AUC (Area Under the Curve) provides the area under this curve as a measure of the overall performance of the classifier. As the ROC is based on a binary classification system, the abnormal BPM (17 onward) is labeled as class 0, and the normal BPM (12 to 16) and as class 1. Fig. 11 provides the ROC and AUC (Area Under Curve) of the classes for the binary classification problem. The ROC curve of the classes is different, but the AUC is the same. That identifies that the two classes have achieved the same level of performance but in different ways.

VIII. CONCLUSION

This research developed a novel DT model (ResDT) based on Wi-Fi Carrier State Information (CSI), improved signal processing, and Machine Learning (ML) algorithms for monitoring and classification (binary and multi-class) of patient respiration.

Multiple pre-processing techniques of DC-offset removal, smoothing filter, multiple IIR bandpass filters along with

wavelet decomposition, and Principal Component Analysis (PCA) for removing noise and dimensionality reduction were implemented on the patient respiration data acquired with ESP32 Wi-Fi CSI. Multiple IIR filters and wavelet comparison is provided in the ResDT model to choose the optimal denoising technique for the sensor data. The elliptic filter provides the most accurate Breaths Per Minute (BPM) calculation in the ResDT model by 87.5% as compared to Butterworth (62.5%), Chebyshev 1(75%), Chebyshev 2(68.75%), and wavelet (75%). PCA is compare with Empirical Mode Decomposition (EMD), Single Variable Decomposition (SVD), EMD-PCA in terms of dimensionality reduction of data for the estimation of patient's BPM.

ML supervised learning classification algorithms accuracies, multi-class and binary class with 10-fold cross-validation, are provided for the proposed ResDT model. This provides an overview of the algorithm's accuracies in terms of multi-class and binary-class classification of BPM in decision-making for healthcare professionals. Among the implemented algorithms, fine tree algorithm provides binary and multi-class classification accuracies of 96.9% and 95.8%.

In our research of the proposed ResDT model, the performance accuracies of ML algorithms with k-fold cross-validation are indeed high but k-fold cross-validation is tested as the first validation method for the ResDT model. There is a need to implement and test multiple validation methodologies and big data of the subject's respiration to completely evaluate ML algorithms in the ResDT model. Not only that, with big respiration data (experimental or synthetic generated), multi feature analysis along with ML algorithm implementation on a larger training data.

REFERENCES

[1] T. Wuest, C. Irgens, and K.-D. Thoben, "An approach to monitoring quality in manufacturing using supervised machine learning on product state data," *J. Intell. Manuf.*, vol. 25, no. 5, pp. 1167–1180, Oct. 2014.

[2] I. Lee and K. Lee, "The Internet of Things (IoT): Applications, investments, and challenges for enterprises," *Bus. Horizons*, vol. 58, no. 4, pp. 431–440, Jul. 2015.

[3] M. Rezaei, M. A. Shirazi, and B. Karimi, "IoT-based framework for performance measurement: A real-time supply chain decision alignment," *Ind. Manag. Data Syst.*, vol. 117, no. 4, pp. 688–712, May 2017.

[4] D. Tang, K. Zheng, H. Zhang, Z. Sang, Z. Zhang, C. Xu, J. A. Espinosa-Oviedo, G. Vargas-Solar, and J.-L. Zechinelli-Martini, "Using autonomous intelligence to build a smart shop floor," *Proc. CIRP*, vol. 56, pp. 354–359, Jan. 2016.

[5] M. Karatas, L. Eriskin, M. Deveci, D. Pamucar, and H. Garg, "Big data for healthcare Industry 4.0: applications, challenges and future perspectives," *Exp. Syst. Appl.*, vol. 200, Aug. 2022, Art. no. 116912.

[6] C. Thuemmler and C. Bai, *Health 4.0: How Virtualization and Big Data are Revolutionizing Healthcare*. Berlin, Germany: Springer, 2017.

[7] S. Khan, T. Arslan, and T. Ratnarajah, "Digital twin perspective of fourth industrial and healthcare revolution," *IEEE Access*, vol. 10, pp. 25732–25754, 2022.

[8] F. Tao, Q. Qi, L. Wang, and A. Y. C. Nee, "Digital twin in industry: State-of-the-art," *IEEE Trans. Ind. Informat.*, vol. 15, no. 4, pp. 2405–2415, Apr. 2019.

[9] E. Negri, L. Fumagalli, and M. Macchi, "A review of the roles of digital twin in CPS-based production systems," *Proc. Manuf.*, vol. 11, pp. 939–948, Jan. 2017.

[10] M. Shafto, M. Conroy, R. Doyle, E. Glaessgen, C. Kemp, J. LeMoigne, and L. Wang, "Modeling, simulation, information technology & processing roadmap," *Nat. Aeronaut. Space Admin.*, vol. 32, pp. 1–38, Apr. 2012.

[11] K. Wen, H. Xu, M. Xu, Y. Pei, Y. Lu, H. Zheng, and Z. Li, "Digital twin-driven intelligent control of natural gas flowmeter calibration station," *Measurement*, vol. 217, Aug. 2023, Art. no. 113140.

[12] H. Laaki, Y. Miche, and K. Tammi, "Prototyping a digital twin for real time remote control over mobile networks: Application of remote surgery," *IEEE Access*, vol. 7, pp. 20325–20336, 2019.

[13] H. Elayan, M. Aloqaily, and M. Guizani, "Digital twin for intelligent context-aware IoT healthcare systems," *IEEE Internet Things J.*, vol. 8, no. 23, pp. 16749–16757, Dec. 2021.

[14] J. I. Jimenez, H. Jahankhani, and S. Kendzierskyj, *Health Care in the Cyberspace: Medical Cyber-Physical System and Digital Twin Challenges* (Digital Twin Technologies and Smart Cities). Berlin, Germany: Springer, Jan. 2020.

[15] I. Lee, O. Sokolsky, S. Chen, J. Hatcliff, E. Jee, B. Kim, A. King, M. Mullen-Fortino, S. Park, A. Roederer, and K. K. Venkatasubramanian, "Challenges and research directions in medical cyber-physical systems," *Proc. IEEE*, vol. 100, no. 1, pp. 75–90, Jan. 2012.

[16] N. Dey, A. S. Ashour, F. Shi, S. J. Fong, and J. M. R. S. Tavares, "Medical cyber-physical systems: A survey," *J. Med. Syst.*, vol. 42, no. 4, p. 64, Mar. 2018.

[17] N. Bagaria, F. Laamarti, H. Badawi, A. Albraikan, R. M. Velazquez, and A. E. Saddik, *Health 4.0: Digital Twins for Health and Well-Being*. Berlin, Germany: Springer, 2020.

[18] G. Ahmadi-Assalemi, H. Al-Khateeb, C. Maple, G. Epiphaniou, Z. A. Alhaboby, S. Alkaabi, and D. Alhaboby, "Digital twins for precision healthcare," in *Cyber Defence in the Age of AI, Smart Societies and Augmented Humanity*. Berlin, Germany: Springer, Apr. 2020, pp. 133–158.

[19] R. Martinez-Velazquez, R. Gamez, and A. El Saddik, "Cardio twin: A digital twin of the human heart running on the edge," in *Proc. IEEE Int. Symp. Med. Meas. Appl. (MeMeA)*, Jun. 2019, pp. 26–28.

[20] X. Chen, Y. Feng, W. Zhong, and C. Kleinstreuer, "Numerical investigation of the interaction, transport and deposition of multicomponent droplets in a simple mouth-throat model," *J. Aerosol Sci.*, vol. 105, pp. 108–127, Mar. 2017.

[21] Y. Feng, J. Zhao, X. Chen, and J. Lin, "An in Silico subject-variability study of upper airway morphological influence on the airflow regime in a tracheobronchial tree," *Bioengineering*, vol. 4, no. 4, pp. 90–93, 2017.

[22] X. Chen, Y. Feng, W. Zhong, B. Sun, and F. Tao, "Numerical investigation of particle deposition in a triple bifurcation airway due to gravitational sedimentation and inertial impaction," *Powder Technol.*, vol. 323, pp. 284–293, Jan. 2018.

[23] B. Björnsson, C. Borrebaeck, N. Elander, T. Gasslander, D. R. Gawel, M. Gustafsson, R. Jörnsten, E. J. Lee, X. Li, S. Lilja, D. Martínez-Enguita, A. Matussek, P. Sandström, S. Schäfer, M. Stenmarker, X. F. Sun, O. Sysoev, H. Zhang, and M. Benson, "Digital twins to personalize medicine," *Genome Med.*, vol. 12, no. 1, pp. 1–4, Dec. 2020.

[24] Y. Liu, L. Zhang, Y. Yang, L. Zhou, L. Ren, F. Wang, R. Liu, Z. Pang, and M. J. Deen, "A novel cloud-based framework for the elderly healthcare services using digital twin," *IEEE Access*, vol. 7, pp. 49088–49101, 2019.

[25] N. K. Chakshu, J. Carson, I. Sazonov, and P. Nithiarasu, "A semi-active human digital twin model for detecting severity of carotid stenoses from head vibration—A coupled computational mechanics and computer vision method," *Int. J. Numer. Methods Biomed. Eng.*, vol. 35, no. 5, p. e3180, May 2019.

[26] M. M. Rathore, S. A. Shah, D. Shukla, E. Bentafat, and S. Bakiras, "The role of AI, machine learning, and big data in digital twinning: A systematic literature review, challenges, and opportunities," *IEEE Access*, vol. 9, pp. 32030–32052, 2021.

[27] World Health Organization. *Ageing and Health*. Accessed: May 12, 2023. [Online]. Available: https://www.who.int/news-room/fact-sheets/detail/ageing-and-health#:~:text=Common%20conditions%20in%20older%20age,conditions%20at%20the%20same%20time

[28] V. Atella, A. Piano Mortari, J. Kopinska, F. Belotti, F. Lapi, C. Cricelli, and L. Fontana, "Trends in age-related disease burden and healthcare utilization," *Aging Cell*, vol. 18, no. 1, p. e12861, Feb. 2019.

[29] T. M. Dall, P. D. Gallo, R. Chakrabarti, T. West, A. P. Semilla, and M. V. Storm, "An aging population and growing disease burden will require alarge and specialized health care workforce by 2025," *Health Affairs*, vol. 32, no. 11, pp. 2013–2020, Nov. 2013.

[30] P. Kumar and K. Silambarasan, "Enhancing the performance of healthcare service in IoT and cloud using optimized techniques," *IETE J. Res.*, vol. 68, no. 2, pp. 1475–1484, Aug. 2019.

[31] I. Mistry, S. Tanwar, S. Tyagi, and N. Kumar, "Blockchain for 5G-enabled IoT for industrial automation: A systematic review, solutions, and challenges," *Mech. Syst. Signal Process.*, vol. 135, Jan. 2020, Art. no. 106382.

[32] S. D. Min, J. K. Kim, H. S. Shin, Y. H. Yun, C. K. Lee, and M. Lee, "Noncontact respiration rate measurement system using an ultrasonic proximity sensor," *IEEE Sensors J.*, vol. 10, no. 11, pp. 1732–1739, Nov. 2010.

[33] P. Jagadev and L. I. Giri, "Non-contact monitoring of human respiration using infrared thermography and machine learning," *Infr. Phys. Technol.*, vol. 104, Jan. 2020, Art. no. 103117.

[34] M. Chu, T. Nguyen, V. Pandey, Y. Zhou, H. N. Pham, R. Bar-Yoseph, S. Radom-Aizik, R. Jain, D. M. Cooper, and M. Khine, "Respiration rate and volume measurements using wearable strain sensors," *npj Digit. Med.*, vol. 2, no. 1, p. 8, Feb. 2019.

[35] F. Ryser, S. Hanassab, O. Lambercy, E. Werth, and R. Gassert, "Respiratory analysis during sleep using a chest-worn accelerometer: A machine learning approach," *Biomed. Signal Process. Control*, vol. 78, Sep. 2022, Art. no. 104014.

[36] H. Tang, J. Gao, C. Ruan, T. Qiu, and Y. Park, "Modeling of heart sound morphology and analysis of the morphological variations induced by respiration," *Comput. Biol. Med.*, vol. 43, no. 11, pp. 1637–1644, Nov. 2013.

[37] C. O'Brien and C. Heneghan, "A comparison of algorithms for estimation of a respiratory signal from the surface electrocardiogram," *Comput. Biol. Med.*, vol. 37, no. 3, pp. 305–314, Mar. 2007.

[38] E. P. Doheny, B. P. O'Callaghan, V. S. Fahed, J. Liegey, C. Goulding, S. Ryan, and M. M. Lowery, "Estimation of respiratory rate and exhale duration using audio signals recorded by smartphone microphones," *Biomed. Signal Process. Control*, vol. 80, Feb. 2023, Art. no. 104318.

[39] I. F. Miller, A. D. Becker, B. T. Grenfell, and C. J. E. Metcalf, "Disease and healthcare burden of COVID-19 in the United States," *Nature Med.*, vol. 26, no. 8, pp. 1212–1217, Aug. 2020.

[40] M. Chandra, K. Kumar, P. Thakur, S. Chattopadhyaya, F. Alam, and S. Kumar, "Digital technologies, healthcare and COVID-19: insights from developing and emerging nations," *Health Technol.*, vol. 12, no. 4, pp. 1–22, Mar. 2022.

[41] M. Bartula, T. Tigges, and J. Muehlsteff, "Camera-based system for contactless monitoring of respiration," in *Proc. 35th Annu. Int. Conf. IEEE Eng. Med. Biol. Soc. (EMBC)*, Osaka, Japan, Jul. 2013, pp. 3–7.

[42] A. Jalal, Y.-H. Kim, Y.-J. Kim, S. Kamal, and D. Kim, "Robust human activity recognition from depth video using spatiotemporal multi-fused features," *Pattern Recognit.*, vol. 61, pp. 295–308, Jan. 2017.

[43] M. H. Siddiqi, R. Ali, M. S. Rana, E. K. Hong, E. S. Kim, and S. Lee, "Video-based human activity recognition using multilevel wavelet decomposition and stepwise linear discriminant analysis," *Sensors*, vol. 14, no. 4, pp. 6370–6392, Apr. 2014.

[44] S. Khan, I. M. Saied, T. Ratnarajah, and T. Arslan, "Evaluation of unobtrusive microwave sensors in healthcare 4.0—Toward the creation of digital-twin model," *Sensors*, vol. 22, no. 21, p. 8519, Nov. 2022.

[45] D. Dias and J. P. S. Cunha, "Wearable health devices—Vital sign monitoring, systems and technologies," *Sensors*, vol. 18, no. 8, p. 2414, Jul. 2018.

[46] M. Zhang and A. A. Sawchuk, "Human daily activity recognition with sparse representation using wearable sensors," *IEEE J. Biomed. Health Informat.*, vol. 17, no. 3, pp. 553–560, May 2013.

[47] R. Mafrur, I. G. D. Nugraha, and D. Choi, "Modeling and discovering human behavior from smartphone sensing life-log data for identification purpose," *Hum.-Centric Comput. Inf. Sci.*, vol. 5, no. 1, pp. 1–18, Dec. 2015.

[48] J.-L. Reyes-Ortiz, L. Oneto, A. Samà, X. Parra, and D. Anguita, "Transition-aware human activity recognition using smartphones," *Neurocomputing*, vol. 171, pp. 754–767, Jan. 2016.

[49] J. D. P. Ribeiro Filho, F. J. Da Silva e Silva, L. R. Coutinho, and B. D. T. P. Gomes, "MHARS: A mobile system for human activity recognition and inference of health situations in ambient assisted living," *J. Appl. Comput. Res.*, vol. 5, no. 1, pp. 44–58, Jul. 2016.

[50] X. Hong and C. D. Nugent, "Segmenting sensor data for activity monitoring in smart environments," *Pers. Ubiquitous Comput.*, vol. 17, no. 3, pp. 545–559, Mar. 2013.

[51] Q. Zhou, J. Xing, Q. Yang, Y. Chen, and B. Feng, "Measuring intrinsic human activity information using WiFi-based attention model," *Measurement*, vol. 195, May 2022, Art. no. 111084.

[52] G. Cosoli, S. Spinsante, F. Scardulla, L. D'Acquisto, and L. Scalise, "Wireless ECG and cardiac monitoring systems: State of the art, available commercial devices and useful electronic components," *Measurement*, vol. 177, Jun. 2021, Art. no. 109243.

[53] J. Liu, G. Teng, and F. Hong, "Human activity sensing with wireless signals: A survey," *Sensors*, vol. 20, no. 4, p. 1210, Feb. 2020.

[54] D. Halperin, W. Hu, A. Sheth, and D. Wetherall, "Tool release: Gathering 802.11n traces with channel state information," *ACM SIGCOMM Comput. Commun. Rev.*, vol. 41, no. 1, p. 53, Jan. 2011.

[55] J. Yang, H. Zou, H. Jiang, and L. Xie, "CareFi: Sedentary behavior monitoring system via commodity WiFi infrastructures," *IEEE Trans. Veh. Technol.*, vol. 67, no. 8, pp. 7620–7629, Aug. 2018.

[56] J. Yang, H. Zou, Y. Zhou, and L. Xie, "Learning gestures from WiFi: A Siamese recurrent convolutional architecture," *IEEE Internet Things J.*, vol. 6, no. 6, pp. 10763–10772, Dec. 2019.

[57] Y. Zeng, D. Wu, R. Gao, T. Gu, and D. Zhang, "FullBreathe: Full human respiration detection exploiting complementarity of CSI phase and amplitude of WiFi signals," *Proc. ACM Interact., Mobile, Wearable Ubiquitous Technol.*, vol. 2, no. 3, pp. 1–19, Sep. 2018.

[58] H. Zou, Y. Zhou, J. Yang, W. Gu, L. Xie, and C. J. Spanos, "Wifi-based human identification via convex tensor shapelet learning," in *Proc. 32nd AAAI Conf. Artif. Intell.*, New Orleans LA, USA, Apr. 2018, pp. 1711–1718.

[59] H. Zou, Y. Zhou, J. Yang, W. Gu, L. Xie, and C. Spanos, "FreeDetector: Device-free occupancy detection with commodity WiFi," in *Proc. IEEE Int. Conf. Sens., Commun. Netw. (SECON Workshops)*, San Diego, CA, USA, Jun. 2017, pp. 1–5.

[60] H. Zou, Y. Zhou, J. Yang, and C. J. Spanos, "Device-free occupancy detection and crowd counting in smart buildings with WiFi-enabled IoT," *Energy Buildings*, vol. 174, pp. 309–322, Sep. 2018.

[61] J. Yang, H. Zou, H. Jiang, and L. Xie, "Device-free occupant activity sensing using WiFi-enabled IoT devices for smart homes," *IEEE Internet Things J.*, vol. 5, no. 5, pp. 3991–4002, Oct. 2018.

[62] W. Li, M. J. Bocus, C. Tang, S. Vishwakarma, R. J. Piechocki, K. Woodbridge, and K. Chetty, "A taxonomy of WiFi sensing: CSI vs passive WiFi radar," in *Proc. IEEE Globecom Workshops (GC Wkshps*, Dec. 2020, pp. 1–6.

[63] N. Bao, J. Du, C. Wu, D. Hong, J. Chen, R. Nowak, and Z. Lv, "Wi-breath: A WiFi-based contactless and real-time respiration monitoring scheme for remote healthcare," *IEEE J. Biomed. Health Informat.*, vol. 27, no. 5, pp. 2276–2285, May 2023.

[64] J. Hu, J. Yang, J.-B. Ong, D. Wang, and L. Xie, "ResFi: WiFi-enabled device-free respiration detection based on deep learning," in *Proc. IEEE 17th Int. Conf. Control Autom. (ICCA)*, Jun. 2022, pp. 510–515.

[65] J. Lever, M. Krzywinski, and N. Altman, "Principal component analysis," *Nature Methods*, vol. 14, pp. 641–642, Jun. 2017.

[66] F. Castells, P. Laguna, L. Sörnmo, A. Bollmann, and J. M. Roig, "Principal component analysis in ECG signal processing," *EURASIP J. Adv. Signal Process.*, vol. 2007, no. 1, pp. 1–21, Dec. 2007.

[67] L. Ren, H. Wang, K. Naishadham, O. Kilic, and A. E. Fathy, "Phase-based methods for heart rate detection using UWB impulse Doppler radar," *IEEE Trans. Microw. Theory Techn.*, vol. 64, no. 10, pp. 3319–3331, Oct. 2016.

[68] J. Meng and Y. Yang, "Symmetrical two-dimensional PCA with image measures in face recognition," *Int. J. Adv. Robotic Syst.*, vol. 9, no. 6, p. 238, Dec. 2012.

[69] S. Karamizadeh, S. M. Abdullah, A. A. Manaf, M. Zamani, and A. Hooman, "An overview of principal component analysis," *J. Signal Inf. Process.*, vol. 4, pp. 173–175, Aug. 2013.

[70] P. J. Phillips, P. J. Flynn, T. Scruggs, K. W. Bowyer, J. Chang, K. Hoffman, J. Marques, J. Min, and W. Worek, "Overview of the face recognition grand challenge," in *Proc. IEEE Comput. Soc. Conf. Comput. Vis. Pattern Recognit.*, San Diego, CA, USA, 2005, pp. 947–954.

[71] S. Asadi, C. D. V. S. Rao, and V. Saikrishna, "A comparative study of face recognition with principal component analysis and cross-correlation technique," *Int. J. Comput. Appl.*, vol. 10, no. 8, pp. 17–21, Nov. 2010.

[72] C. Li, Y. Diao, H. Ma, and Y. Li, "A statistical PCA method for face recognition," in *Proc. 2nd Int. Symp. Intell. Inf. Technol. Appl.*, Shanghai, China, Dec. 2008, pp. 376–380.

[73] L. D. Khanh and P. X. Duong, "Principal component analysis for heart rate measurement using UWB radar," *Int. J. FUZZY Log. Intell. Syst.*, vol. 20, no. 3, pp. 211–218, Sep. 2020.

[74] M. A. Motin, C. K. Karmakar, and M. Palaniswami, "Ensemble empirical mode decomposition with principal component analysis: A novel approach for extracting respiratory rate and heart rate from photoplethysmographic signal," *IEEE J. Biomed. Health Informat.*, vol. 22, no. 3, pp. 766–774, May 2018.

[75] A. Garde, W. Karlen, J. M. Ansermino, and G. A. Dumont, "Estimating respiratory and heart rates from the correntropy spectral density of the photoplethysmogram," *PLoS ONE*, vol. 9, no. 1, pp. 1–11, Jan. 2014.

[76] W. Karlen, S. Raman, J. M. Ansermino, and G. A. Dumont, "Multiparameter respiratory rate estimation from the photoplethysmogram," *IEEE Trans. Biomed. Eng.*, vol. 60, no. 7, pp. 1946–1953, Jul. 2013.

[77] A. Garde, W. Karlen, P. Dehkordi, J. Ansermino, and G. Dumont, "Empirical mode decomposition for respiratory and heart rate estimation from the photoplethysmogram," in *Proc. Comput. Cardiol.*, Zaragoza, Spain, Sep. 2013, pp. 22–25.

[78] T. Kanda, T. Sato, H. Awano, S. Kondo, and K. Yamamoto, "Respiratory rate estimation based on WiFi frame capture," in *Proc. IEEE 19th Annu. Consum. Commun. Netw. Conf. (CCNC)*, Jan. 2022, pp. 881–884.

[79] P. Langley, E. J. Bowers, and A. Murray, "Principal component analysis as a tool for analyzing beat-to-beat changes in ECG features: Application to ECG-derived respiration," *IEEE Trans. Biomed. Eng.*, vol. 57, no. 4, pp. 821–829, Apr. 2010.

[80] D. Widjaja, C. Varon, A. Dorado, J. A. K. Suykens, and S. Van Huffel, "Application of kernel principal component analysis for single-lead-ECG-derived respiration," *IEEE Trans. Biomed. Eng.*, vol. 59, no. 4, pp. 1169–1176, Apr. 2012.

[81] N. U. Rehman and D. P. Mandic, "Empirical mode decomposition for trivariate signals," *IEEE Trans. Signal Process.*, vol. 58, no. 3, pp. 1059–1068, Mar. 2010.

[82] P. Trnka and M. Hofreiter, "The empirical mode decomposition in real-time," in *Proc. 18th Int. Conf. Process Control*. Tatranská Lomnica, Slovakia: Slovak Univ. of Technology in Bratislava, 2011, pp. 14–17.

[83] S. A. Anapagamini and R. Rajavel, "Removal of artifacts in ECG using empirical mode decomposition," in *Proc. Int. Conf. Commun. Signal Process.*, Melmaruvathur, India, Apr. 2013, pp. 288–292.

[84] E. Pinheiro, O. Postolache, and P. Girão, "Empirical mode decomposition and principal component analysis implementation in processing non-invasive cardiovascular signals," *Measurement*, vol. 45, no. 2, pp. 175–181, Feb. 2012.

[85] S. Hadiyoso, E. M. Dewi, and I. Wijayanto, "Comparison of emd, vmd and eemd methods in respiration wave extraction based on ppg waves," in *Proc. 2nd Int. Conf. Electron. Represent. Algorithm 'Innovation Transformation Best Practices Global Community'*, Yogyakarta, Indonesia, Dec. 2019, pp. 12–13.

[86] A. Karagiannis, L. Loizou, and P. Constantinou, "Experimental respiratory signal analysis based on empirical mode decomposition," in *Proc. 1st Int. Symp. Appl. Sci. Biomed. Commun. Technol.*, Aalborg, Denmark, Oct. 2008, pp. 1–5.

[87] S. Liu, Q. Qi, H. Cheng, L. Sun, Y. Zhao, and J. Chai, "A vital signs fast detection and extraction method of UWB impulse radar based on SVD," *Sensors*, vol. 22, no. 3, p. 1177, Feb. 2022.

[88] Y. Wang and L. Zhu, "Research and implementation of SVD in machine learning," in *Proc. IEEE/ACIS 16th Int. Conf. Comput. Inf. Sci. (ICIS)*, Wuhan, China, May 2017, pp. 471–475.

[89] Alzaabi, T. Arslan, and N. Polydorides, "Respiration rate measurement validity and repeatability of ubiquitous non-contact Wi-Fi sensing for older adults in care," *IEEE Dataport*, Jun. 2022.

[90] S. Mosleh, J. B. Coder, C. G. Scully, K. Forsyth, and M. O. A. Kalaa, "Monitoring respiratory motion with Wi-Fi CSI: Characterizing performance and the BreatheSmart algorithm," *IEEE Access*, vol. 10, pp. 131932–131951, 2022.

[91] S. Rani, A. Kaur, and J. Ubhi, "Comparative study of FIR and IIR filters for the removal of Baseline noises from ECG signal," *Int. J. Comput. Sci. Inf. Technol.*, vol. 2, no. 3, pp. 1105–1108, 2011.

[92] G. B. Drummond, D. Fischer, and D. K. Arvind, "Current clinical methods of measurement of respiratory rate give imprecise values," *ERJ Open Res.*, vol. 6, no. 3, pp. 00023–2020, Jul. 2020.

[93] M. Piotrowski and M. Derén, "Towards the development of a patient monitoring system: Review of available solutions and assumptions for building a functionally optimal system," *Polish J. Aviation Med., Bioeng. Psychol.*, vol. 26, no. 1, pp. 26–34, Mar. 2023.

[94] N. Rubio, R. A. Parker, E. M. Drost, H. Pinnock, C. J. Weir, J. Hanley, L. C. Mantoani, W. MacNee, B. McKinstry, and R. A. Rabinovich, "Home monitoring of breathing rate in people with chronic obstructive pulmonary disease: Observational study of feasibility, acceptability, and change after exacerbation," *Int. J. Chronic Obstructive Pulmonary Disease*, vol. 12, pp. 1221–1231, Apr. 2017.

[95] D. J. Bartholomew, *Principal Components Analysis*. Amsterdam, The Netherlands: Elsevier, 2010.

[96] B. Yu, Y. Wang, K. Niu, Y. Zeng, T. Gu, L. Wang, C. Guan, and D. Zhang, "WiFi-sleep: Sleep stage monitoring using commodity Wi-Fi devices," *IEEE Internet Things J.*, vol. 8, no. 18, pp. 13900–13913, Sep. 2021.

[97] A. Holzinger, "Big data calls for machine learning," *Encyclopedia Biomed. Eng.*, vol. 3, pp. 258–264, 2019.

[98] E. J. Topol, "High-performance medicine: The convergence of human and artificial intelligence," *Nature Med.*, vol. 25, no. 1, pp. 44–56, Jan. 2019.

[99] I. Al-Zyoud, F. Laamarti, X. Ma, D. Tobon, and A. E. Saddik, "Towards a machine learning-based digital twin for non-invasive human bio-signal fusion," *Sensors*, vol. 22, p. 7457, Dec. 2022.

[100] L. Zhou, S. Pan, J. Wang, and A. V. Vasilakos, "Machine learning on big data: Opportunities and challenges," *Neurocomputing*, vol. 237, pp. 350–361, May 2017.

[101] A. Vabalas, E. Gowen, E. Poliakoff, and A. J. Casson, "Machine learning algorithm validation with a limited sample size," *PLoS ONE*, vol. 14, no. 11, Nov. 2019, Art. no. e0224365.

SAGHEER KHAN received the bachelor's degree in electrical, with a focus on electronics from the Army Public College of Management and Sciences (APCOMS), University of Engineering and Technology (UET), Taxila, Pakistan, in 2016, and the master's degree in electrical engineering, with a focus on communication and signal processing from the National University of Sciences and Technology (NUST), Islamabad, Pakistan, in 2019. He is currently pursuing the Ph.D. degree with the Scottish Microelectronic Centre (SMC), School of Engineering, The University of Edinburgh. His research interests include digital twin (DT), industry 4.0, 5G, and the IoT.

AAESHA ALZAABI (Member, IEEE) received the B.Sc. degree in electrical engineering from the American University of Sharjah, United Arab Emirates, in 2017, and the M.Sc. degree in signal processing and communications from The University of Edinburgh, in 2020, where she is currently pursuing the Ph.D. degree in engineering with the Institute for Integrated Micro and Nano Systems. Her research interests include RF sensing, wireless communications, embedded systems, and sensor fusion.

ZAFAR IQBAL received the bachelor's degree from the University of Engineering and Technology (UET), Lahore, Pakistan, and the master's degree in power systems and its automation from North China Electric Power University, Beijing. He is currently pursuing the Ph.D. degree with the Institute of Energy Systems, School of Engineering, The University of Edinburgh, Edinburgh. His bachelor's degree thesis focused on design, implementation and monitoring of photovoltaic system. He was a Research Assistance in multi-vector mini-grid analysis and modeling with The University of Edinburgh, from October 2022 to February 2023. He performed the duties of a Lecturer with the University of Management and Technology, Lahore, from October 2017 to July 2018. His research interests include electrical power systems, grid-connected inverters, and machine learning.

THARMALINGAM RATNARAJAH (Senior Member, IEEE) is currently with the Institute for Digital Communications, The University of Edinburgh, Edinburgh, U.K., as a Professor of digital communications and signal processing. He was the Head of the Institute for Digital Communications, from 2016 to 2018. He has supervised 16 Ph.D. students and 21 postdoctoral research fellows and raised more than 11 million USD of research funding. He was a Coordinator of the EU Projects ADEL (3.7M€) in the area of licensed shared access for 5G wireless networks, HARP (4.6M€) in the area of highly distributed MIMO, and EU Future and Emerging Technologies Projects HIATUS (3.6M€) in the area of interference alignment, and CROWN (3.4M€) in the area of cognitive radio networks. His research interests include signal processing and information theoretic aspects of 6G wireless networks, full-duplex radio, mmwave communications, random matrices theory, interference alignment, statistical and array signal processing, and quantum information theory. He has published over 400 publications in these areas and holds four U.S. patents. He is a fellow of the Higher Education Academy (FHEA). He was the Technical Co-Chair of the 17th IEEE International workshop on Signal Processing advances in Wireless Communications, Edinburgh, U.K., in July 2016. He was an Associate Editor of IEEE TRANSACTIONS ON SIGNAL PROCESSING, from 2015 to 2017.

TUGHRUL ARSLAN (Senior Member, IEEE) holds the Chair of integrated electronic systems with the School of Engineering, The University of Edinburgh, Edinburgh, U.K. He is a member of the Integrated Micro and Nano Systems (IMNS) Institute, and leads the Embedded Mobile and Wireless Sensor Systems (Ewireless) Group with the University (ewireless.eng.ed.ac.uk). He is the author of more than 500 refereed articles and an inventor of more than 20 patents. His research interest includes developing low power radio frequency sensors for wearable and portable biomedical applications. He has been a member of the IEEE CAS Executive Committee on VLSI Systems and Applications, since 1999, and the steering and technical committees of a number of international conferences. He is a Co-Founder of the NASA/ESA Conference on Adaptive Hardware and Systems (AHS) and currently serves as a member for its steering committee. He is an Associate Editor of the IEEE TRANSACTIONS ON VERY LARGE SCALE INTEGRATION (VLSI) SYSTEMS. Previously, he was an Associate Editor of the IEEE TRANSACTIONS ON CIRCUITS AND SYSTEMS—I: REGULAR PAPERS, from 2005 to 2006, and IEEE TRANSACTIONS ON CIRCUITS AND SYSTEMS—II: EXPRESS BRIEFS, from 2008 to 2009.